Research Journal of Physical Sciences ISSN 2320–4796
Vol. **3(6),** 16-19, August **(2015)** *Res. J. Physical Sci.*

Effect of Reactant concentration on Structural and Optical properties of ZnS - PVA nanocomposite

Deka D.C. and Bordaloi S.
Department of Instrumentation and USIC, Gauhati University, Guwahati -781014, Assam, INDIA

Available online at: www.isca.in
Received 22nd June 2015, revised 8th July 2015, accepted 2nd August 2015

Abstract

ZnS-PVA nanocomposite thin films are deposited on glass substrate by chemical route. Effect of reactant concentration on the as synthesized ZnS-PVA nanocomposites are studied by taking three different concentrations of zinc source keeping the sulphur source concentration fixed. For structural and morphological studies the as synthesized thin films are characterized by using XRD and TEM. The X-ray diffractogram of the samples show wurtzite structure with preferred orientations along (002), (110) and (112) planes. The crystallite sizes of the films are found to vary from 3.54 - 4.09 nm which are in good agreement with TEM results. The bandgap of the synthesized nanomaterials are calculated using UV- visible spectral analysis and bandgap plot. The bandgap value is found to be within the range 3.7-3.8eV. Also we have used photoluminescence study to identify the defects in the nanostructure.

Keywords: Nanostructure, TEM, Photoluminescence.

Introduction

Nanomaterials are studied extensively because they show very different properties compared to what they exhibit in bulk form[1-3]. For example as the size of the system decreases, the quantum size effect becomes pronounced where the electronic properties of the solid are altered. Meanwhile, the increase of surface to volume ratio changes the mechanical, thermal and catalytic properties of the material significantly. The distinct properties enable unique applications of nanomaterials. As an important II-VI group semiconductor material, ZnS has been intensively studied because of its wide application in optical sensor, photo catalysts in environmental protection, light emitting diodes, electroluminescence devices, photovoltaic devices, lasers, single electron transistors as well as biological sciences and diagnostics[4-11]. ZnS has wide bandgap of 3.68 eV at room temperature. This bandgap can be enhanced by decreasing the sizes of the crystallites.

Here, we report the synthesis of ZnS nanocrystal in the polyvinyl alcohol (PVA) solution by chemical route for different concentrations of Zinc source keeping that of Sulphur source fixed. PVA is a hydrophilic polymer frequently used as a matrix for stabilization of ZnS nanocrystal extensively[11-12]. In this paper an attempt is made to correlate the structural parameters with molarities of reactant.

Material and Methods

Nanocrystalline ZnS-PVA composite thin films are deposited on glass substrate by chemical route at 90^0C. The synthesis is carried out as follows- $1.33x10^{-5}$ M of PVA is stirred in 75 ml distilled water for 1.5hr with temperature controlled magnetic stirrer. Then the PVA solution is kept at rest for 2 hrs. A solution of 0.005 M zinc acetate in 5 ml $NH_4(OH)$ is mixed to the PVA solution. Lastly, a solution prepared by taking 0.015M Na_2S in 25 ml distilled water is added to the above solution. Then the resulting mixture is heated to the temperature 90^0C and kept at that temperature for 20 minutes. The solution containing ZnS-PVA is cast over glass substrates to produce thin film form. The above procedure is repeated for three different concentrations of Zinc source keeping the concentration of sulphur source fixed.

After deposition, the films are dried in vacuam and set for various characterizations. Structural characterizations of the films are determined by Philips X'pert prodiffractometer (PW-1830) at room temperature with CuK_α (1.54A°) radiation. Morphological studies are carried out using Transmission Electron Microscope (JEM 100CXII JEOL, Japan). Optical transmission spectra of the films are taken with the help of a UV Spectrometer (Hitachi U-3210 Spectrometer). Photoluminescence spectra are recorded by Hitachi F-2500 Fluorescence Spectrometer.

Results and Discussion

XRD Study: X-ray diffractogram of the ZnS-PVA nanocomposite thin films for different concentrations of $Zn(CH_3COO)_2$ keeping the concentration of Na_2S fixed are shown in figure-1. X-ray diffractogram of the films show in fig. 1 exhibit broadened diffraction profiles confirming formation of ZnS nanocrystal. The analysis of the profile shows preferred orientations along (002), (110) and (112) planes. The crystallite size (D) of the Nanocrystalline films are estimated by using Debye-Scherrer formula

$D=0.89\lambda/\beta\cos\theta$ (1)

where λ, β and θ are the wavelength of the CuK_α radiation (1.54A°), full width at half maximum of the diffraction peak and diffraction angle respectively. The values of the crystallite sizes of the synthesized ZnS nanoparticles are found to be 3.54 nm, 3.76 nm and 4.09 nm for the three concentrations of $Zn(CH_3COO)_2$ as.005 M, 0.0065 M and 0 .008 M respectively. n

Thus it is seen that the crystallite size increases with increase in concentration of Zn source.

TEM Study: The size and morphology of the ZnS-PVA nanocomposite thin films are examined by taking TEM images of the synthesized nanocomposite thin films and are shown in figure-2(a), 2(b) and 2(c). TEM micrographs show spherical particles of nearly uniform size.

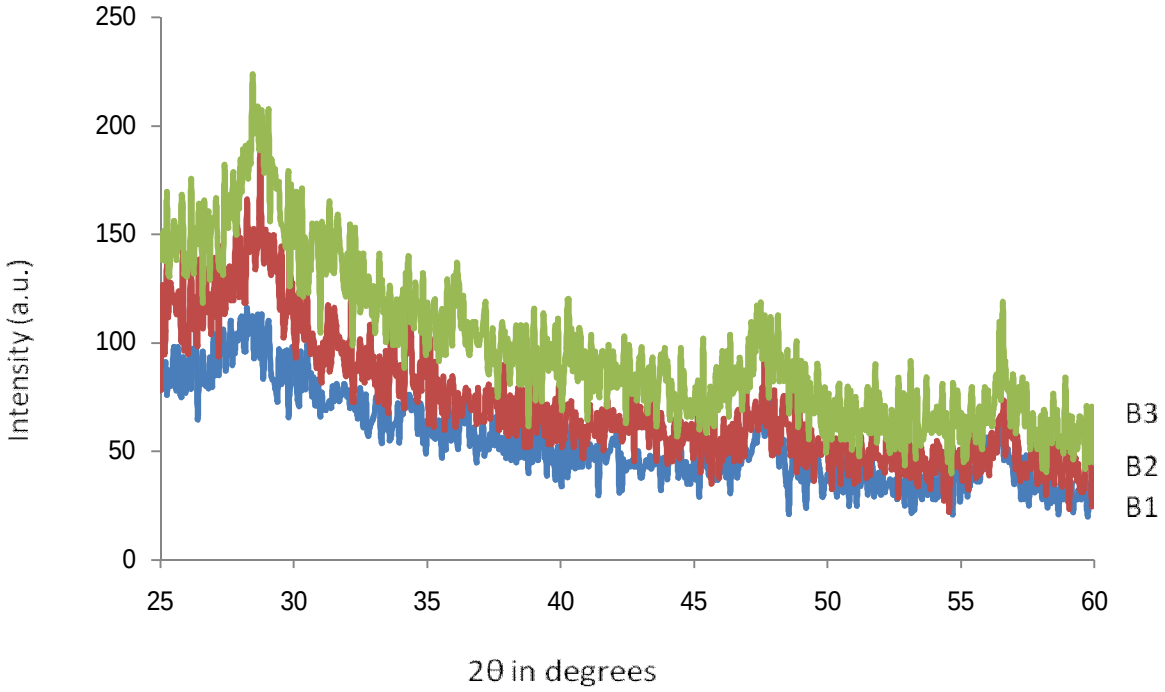

Figure-1
X-ray diffraction (XRD) pattern of the ZnS-PVA nanocomposite thin films for concentrations (B_1) .005 M (B_2).0065 M and (B_3).008 M of $Zn(CH_3COO)_2$ keeping that of Na_2S fixed

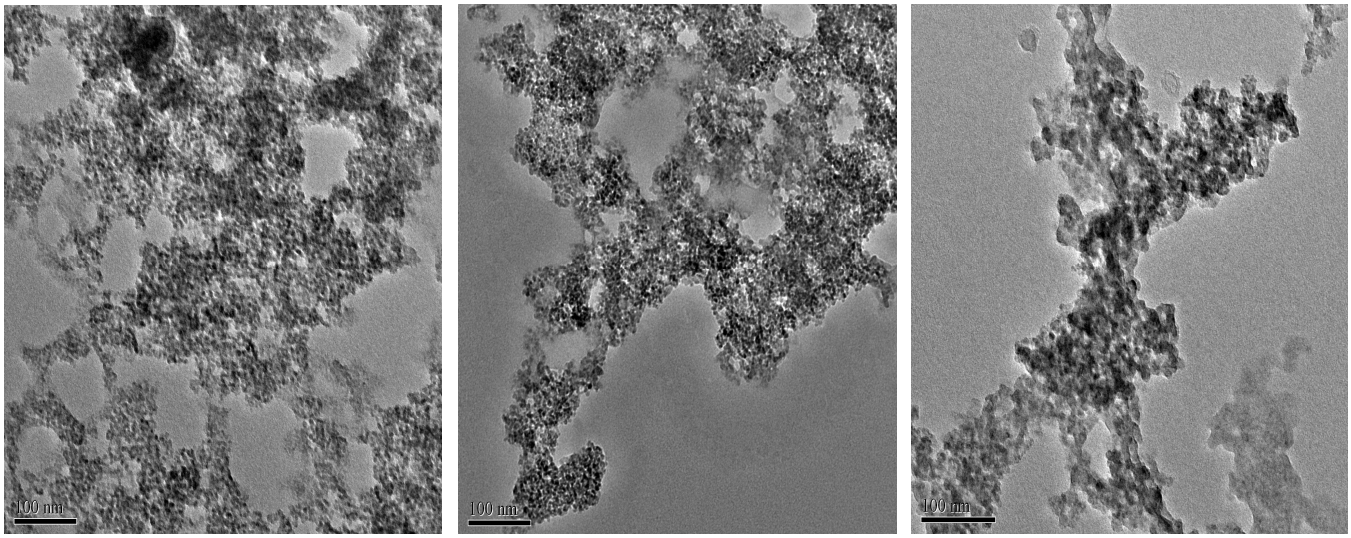

B1 B2 B3

Figure-2
(a), 2(b), 2(c) TEM images of the samples B_1, B_2 and B_3 respectively

The average particle sizes from TEM are calculated as 6.10 nm, 8.62 nm and 11.85 nm respectively for the three concentrations of $Zn(CH_3COO)_2$ as.005 M, 0.0065 M and 0 .008 M respectively .The particle size obtained from XRD and TEM may be different[13] for various reasons. One of the reasons is that the peak broadening may be caused by inhomogeneous strains, twinned structures, lattice bending or other point defects in the crystal.

Optical Absorption Study: Optical studies of the synthesized ZnS-PVA nanocomposite thin films are carried out by measuring the transmittance as a function of wavelength. Fig. 3(a) shows the transmittance (T) versus wavelength (λ) spectra of the as deposited films.

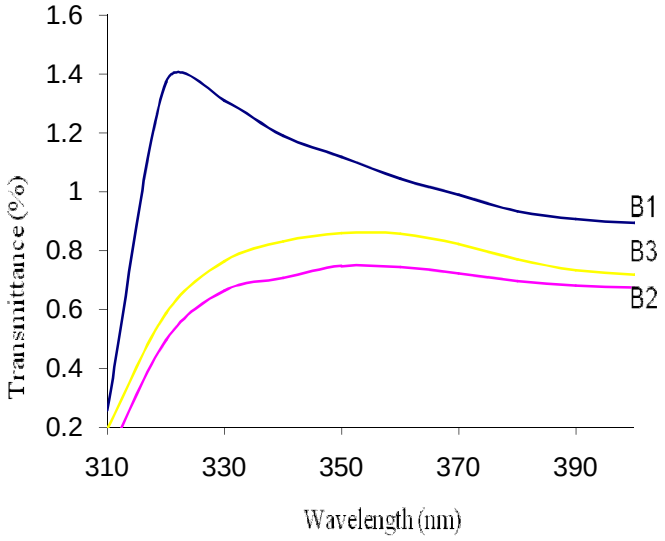

Figure-3(a)
UV-visible transmittance as a function of wavelength for the samples B_1, B_2 and B_3 respectively

The relation between absorption coefficient (α) and incident photon energy (hυ) can be written as

$$\alpha = A\,(h\upsilon - Eg)^n/h\upsilon \qquad (2)$$

where A is a constant, Eg is the band gap of the material and the exponent n depends on the type of transition. The values of n for direct allowed, indirect allowed, direct forbidden transition are n = ½, 2 and 3/2 respectively. Graphs between $(\alpha h\upsilon)^2$ versus (hυ) plotted for different films are shown in figure-3(b) and the intercepts of the extrapolated straight line at $(\alpha h\upsilon)^2 = 0$ gives the direct band gap Eg of the material. The values of Eg are obtained as 3.80 eV, 3.75 eV and 3.70 eV respectively for the three concentrations of $Zn(CH_3COO)_2$ indicating increase in bandgap with decrease in crystallite size.

The blue shift of the bandgap (ΔE_g) may be used to determine the crystallite radius using the relation[14].

$$\Delta E_g = E_g(\text{film}) - E_g(\text{bulk}) = [\,\hbar^2\pi^2/2\mu r^2\,] - [1.8e^2/\epsilon r\,] \qquad (3)$$

where m_e^* and m_h^* are the effective masses of electrons and holes, $\mu = m_e^* m_h^*/(m_e^* + m_e^*)$ is the reduced electron-hole effective mass and ϵ is the dielectric constant of the material. In our study we have taken $m_e^* = 0.34m_o$, $m_h^* = 0.23m_o$, m_o being the free electron mass and ϵ=8.76 (Landolt-Bornstein 1987).

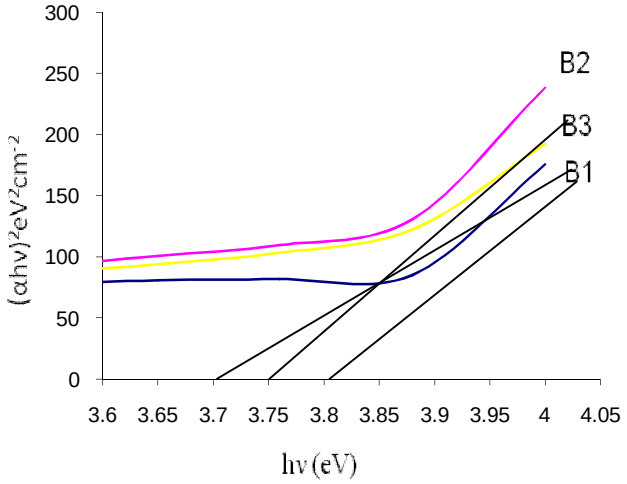

Figure-3(b)
Variation of $(\alpha h\upsilon)^2$ as a function of hυ for direct band gap for the samples B_1, B_2 and B_3 respectively

Using equation (3) we have estimated the particle sizes as 4.35 nm, 5.69 nm and 10.66 nm for the three samples. This result also indicates that the particle size increases with increase in concentration of $Zn(CH_3COO)_2$.

Photoluminescence: Figure-4 shows Photoluminescence spectra of the nanocrystalline ZnS-PVA nanocomposite thin films measured at room temperature (290K). The excitation wavelength is selected as 260 nm. The spectra show a small peak around (430- 450) nm and a broad peak around (500– 520) nm. Denzier et al reported that a strong blue emission around 450nm is due to ZnS multicore microcables and they assigned the peak.

To the defect related emission of ZnS. For ZnS nanobelts Sulieman et al (2006) reported three broad emission peaks at 340 nm, 410 nm and 510 nm. They assigned the peak at 340nm due to the spontaneous emission due to band to band transition, while the 410 nm peak originated from the surface states and 510 nm was attributed to the sulphur vacancies in the single crystal. Borse et al[15] attributed an emission peak at 425 nm observed in the case of nanoparticles of cubic ZnS to sulphur vacancies. Lu et al[16] also reported a peak at 422 nm is due to sulphur vacancies. Based on these reports, the peaks at observed (430 – 450) nm observed in the present study can be assigned to sulphur vacancies i.e. to the recombination of electrons at the sulphur vacancy with holes at the valence band[17]. Also the peak centered at (500–520) nm may be attributed to the stochiometric defects, which might be a vacancy or an interstitial state[18].

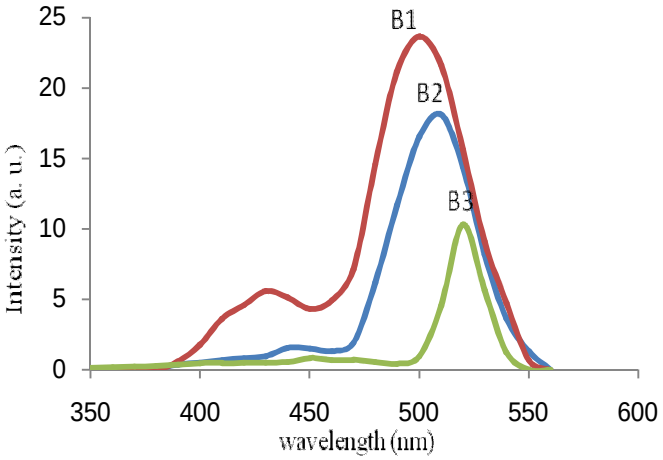

Figure-4
Room temperature PL emission spectra for the samples B_1, B_2 and B_3 respectively

Conclusion

ZnS-PVA nanocomposite thin films have been successfully synthesized by chemical route. From experimental results it is seen that the size and bandgap of the synthesized nanoparticles depends on the reactant concentrations. With increase in zinc source concentration, the size of the nanoparticles increases whereas the bandgap decreases.

Acknowledgements

The authors would like to acknowledge Department of Instrumentation and USIC, Gauhati University for XRD measurements, SAIF, NEHU Shillong for TEM measurements and Department of Chemistry, Gauhati University for UV-visible and PL measurements.

References

1. Tang H., Yan M., Zang H., Xia M., and Yang D., Preparation and characterization of water-soluble CdS nanocrystals by surface modification of ethylene diamine, *Mater. Letts.*, **59,** 1024-1027**(2005)**
2. He R., Qian X., Yin J., Bian L., Xi H. and Zhu Z., In situ synthesis of CdS/PVK nanocomposites and their optical properties, *Mater. Letts.* **57,** 1351-1354**(2003)**
3. Yao K. X., Sinclair R. and Zeng H. C., Symmetric Linear Assembly of Hourglass-like ZnO Nanostructures, *Journal of Physical Chemistry*, **11,** 2032-2039 **(2007)**
4. Hamanoi O. and Kudo A., Reduction of Nitrate and Nitrite Ions over Ni-ZnS Photocatalyst under Visible Light Irradiation in the Presence of a Sacrificial Reagent. *Chem. Lett.*, 838-839 **(2002)**
5. Kudo A. and Sekizawa M., Photocatalytic H2 evolution under visible light irradiation on Ni-doped ZnS photocatalyst, *Chem. Commun.*, 1371-1372 **(2000)**
6. Arai T., Senda S. I., Sato Y.,Takahashi H., Shinoda K., Jeyadevan B. and Tohji K., Cu-Doped ZnS Hollow Particle with High Activity for Hydrogen Generation from Alkaline Sulfide Solution under Visible Light, *Chem. Mater.*, **20,** 1997-2000 **(2008)**
7. Muruganandham M. and Kusumoto Y., Synthesis of N, C codoped hierarchical porous microsphere ZnS as a visible light-responsive photocatalyst, *J. Phys. Chem.*, **C**, **113,** 16144-16150 **(2009)**
8. Kontsogeorgis D. C., Mastoo E. A., Cranton W. M. and Trmas C. B., Pulsed KrF laser annealing of ZnS: Mn laterally emitting thin film electroluminescent displays, *Thin Solid Films*, **383,** 31-33 **(2001)**
9. Pyun J. and Matyjaszewski K., Synthesis of nanocomposite organic/inorganic hybrid materials using controlled/“living” radical polymerization, *Chem. Mater.*, **13,** 3436-3448 **(2001)**
10. Hang J., Oh M. O., Kim I., Lee J. K. and Ha C. S., Preparation and characterization of ZnS based nano-crystalline particles for polymer light-emitting diodes, *Current Appl. Phys.*, **5,** 31-34 **(2005)**
11. Qian X.F., Yin J., Guo X.X., Yang Y.F., Zhu Z.K., Lu., Polymer-inorganic nanocomposites prepared by hydrothermal method: PVA/ZnS, PVA/CdS, preparation and characterization, *J. Mater. Sci. Lett.*, **19,** 2235 **(2000)**
12. Sang W., Qian Y., Min J., Li D., Wang L., Shi W., Yinfeng L., Microstructural and optical properties of ZnS: Cu nanocrystals prepared by an ion complex transformation method, *Solid State Commun.*, **121,** 475 **(2002)**
13. Cao G., Nanostructure and Nanomaterials (London Imperial College Press), **330 (2004)**
14. Yuang Y.S., Chen F.Y., Lee Y.Y. and Liu C.L., J. Photothermal deflection and photoluminescence studies of CdS and CdSe quantum dots, *Appl. Phys.*, **76,** 3041, **(1994)** Japan.
15. Borse P.H., Deshmukh N., Shinde R.F., Date S.K. and Kulkarni S.K., Luminescence quenching in ZnS nanoparticles due to Fe and Ni doping , *J. mater. Sci.*, **34,** 6087 **(1999)**
16. Lu H.Y., Chu S.Y. and Tan S.S., The characteristics of low-temperature-synthesized ZnS and ZnO nanoparticles, *J. Cryst. Growth*, **269,** 385 **(2004)**
17. Sarvana S. Kumar, Abdul M. Khadar, Dhara S.K., Rabindran T. R. and Nair K.G.M., Photoluminescence and Raman studies of ZnS nanoparticles implanted with Cu+ ions, *Nucl. Instr. and Meth. In Phys. Res.***, B, 251,** 435-440 **(2006)**
18. Senthilkumaar S. and Thamiz R. Selvi, Formation and photoluminescence of zinc sulfide nanorods, *J. Appl. Sci.*, **8 (12),** 2306-2311**(2008)**